Transient Stability Analysis of Power Systems using Koopman Operators

Hyungjin Choi Subhonmesh Bose

***Abstract*—We study a Koopman operator based framework to estimate the region of attraction (ROA) of power system dynamics following a line or generator failure. Koopman operators are infinite-dimensional linear operators that can describe the evolution of a nonlinear dynamical system. They admit finite-dimensional approximations that can be learnt from data. The spectral properties of these approximations capture the desired ROA—the object of interest in transient stability analysis. Our numerical results on a 3-bus power system example showcases the power of Koopman operators for transient stability analysis.**

I. Introduction

Transient stability analysis of a power system seeks to answer the question: will grid dynamics converge to a stable equilibrium point, following a line fault or a generator failure? Nonlinearity of the power system dynamics poses a fundamental challenge to the development of analytical and scalable computational tools for such studies.

Transient stability analysis is a mature field of research. Proposed methods vary in their degrees of scalability. In this paper, we argue that Koopman operators can be useful to compute the domain of attraction of post-fault power system dynamics. Based on the intuition derived from Koopman operator theory, we propose a naive approach to estimate that boundary and compute critical clearing times (CCTs) of various faults. Koopman operators, developed in [1], lifts the finite-dimensional nonlinear evolution of the state to a linear but infinite-dimensional evolution of the function space of observables (mappings of the state) [2]–[6]. The proposed method computes a finite-dimensional approximation of these operators [7]–[9], the spectral properties of which contain the information relevant to the region of attraction (ROA) of the post fault dynamics.

Prior literature on transient stability analysis is extensive; see [10]–[12] for surveys. Time-domain simulation is the simplest and the most widely used technique for such analysis. It does so via the computation of state trajectories through numerical integration [12]. Dynamic variations in solar and wind power output, however, require the computation of a large number of trajectories to provide stability guarantees. Despite its simplicity, such requirements render time-domain simulation unsuitable for power systems with increasing penetration of variable renewable supply.

Direct methods for transient stability analysis seek to characterize the region of attraction using sublevel sets of Lyapunov-style functions for power system dynamics. A Lyapunov function decreases along the system trajectory. Therefore, system states can never escape its sublevel sets [13], [14]. Transient Energy Functions (TEF), expounded in [15]–[18], are examples of Lyapunov-style functions that provide stability guarantees for a class of power system models. TEF methods suffer from two limitations. First, TEFs are only known for a limited class of power system models. Second, even when they are known, computation of ROA from TEFs requires knowledge of the critical potential energy at the boundary of the ROA. The controlling Unstable Equilibrium Point (UEP), and closest UEP in [19]–[22] have been proposed to compute that energy. These methods are generally computationally intensive and often yield conservative ROA estimates. Relevant work also includes Boundary Controlling Unstable (BCU) Equilibrium Point method in [16] which improved computational efficiency compared to other methods and has found applicability in practical power systems [23].

Authors in [24]–[27] have proposed to compute Lyapunov functions for power system dynamics using polynomial optimization, following the seminal work of Parrilo in [14]. While promising in theory, state-of-art software for these methods do not scale favorably with the size of the power system. This work reveals the power of Koopman operators in transient stability analysis for power systems. We acknowledge prior contributions of [28], [29] among others that have utilized Koopman operators for power system stability assessment.

In Section II, we introduce Koopman operator theory and in Section III, we describe an approach to estimate the ROA of a power system and study it on a 3-bus power system example in Section IV. Concluding remarks and directions for future work are outlined in Section V.

II. Koopman operator theory

In this section, we introduce Koopman operator theory for power system dynamics, and outline the procedure to compute its finite-dimensional approximation. The next section builds on this approximation to compute the region of attraction for post-fault dynamics of a power system. Throughout this paper, we use the notation $\mathbb{R}$ and $\mathbb{C}$ to denote the sets of real and complex numbers, respectively.

The electromechanical dynamics of a power system can be collectively described by differential alegebraic equations (DAEs). Power flow equations for the network define the algebraic equations. Using Kron reduction as in [30], one can obtain a nonlinear ordinary differential equation (ODE) description of the system dynamics as in [31] of the form $\dot{\mathbf{x}} = \mathbf{f}(\mathbf{x})$. Here, $\mathbf{x} \in \mathbb{R}^n$ denotes the vector of dynamic states that includes machine states such as generator rotor angles/speeds, and controller states associated with the governor, voltage regulator, etc.

H. Choi and S. Bose are with the Department of Electrical and Computer Engineering, University of Illinois at Urbana-Champaign, Urbana, IL 61801, USA. Email: {hjchoi12, boses}@illinois.edu.

We discretize the ODE with time step Δ to obtain

$$\mathbf{x}_{t+1} = \mathbf{F}(\mathbf{x}_t) \tag{1}$$

for $t \geq 0$. We choose Δ smaller than the least time constant of the continuous-time system, but large enough to show appreciable change in the states in each time step. Assume henceforth that $\mathbf{F}$ describes the discretized grid dynamics following a contingency.

A. Koopman Operator and its Spectral Decomposition

Our description of Koopman operator theory largely mirrors that in [7]. Define an observable g as a complex map on the state space $\mathbb{X}$, i.e., $g : \mathbb{X} \to \mathbb{C}$. In the sequel, let $\mathbb{G}$ denote the space of all L_2-measurable observables. Then, Koopman operator $\mathcal{K} : \mathbb{G} \to \mathbb{G}$ propagates an observable g through the system dynamics, i.e., $\mathcal{K}g = g \circ \mathbf{F}$. In other words, we have

$$\mathcal{K}g(\mathbf{x}) = g(\mathbf{F}(\mathbf{x})). \tag{2}$$

The above definition implies that $\mathcal{K}$ is a linear but infinite-dimensional operator. Instead of the nonlinear evolution of states in the finite-dimensional Euclidean space $\mathbb{X}$ governed by $\mathbf{F}$, Koopman operator theory shifts the focus of analysis to the linear evolution of observables in the infinite-dimensional space $\mathbb{G}$ governed by $\mathcal{K}$.

Of interest to us is the spectrum of $\mathcal{K}$ that is useful to compute ROA for power system dynamics following a contingency. Call $\varphi_\lambda : \mathbb{G} \to \mathbb{G}$ an eigenfunction of $\mathcal{K}$ and λ its associated eigenvalue, if

$$\mathcal{K}\varphi_\lambda = \lambda\varphi_\lambda.$$

We are specifically interested in the dynamics of the full state as observables, i.e., stack the n coordinates of the state in $\mathbf{g}(\mathbf{x}) = \mathbf{x}$. Assuming each of them to be within the span of the eigenfunctions, we have

$$\mathbf{x} = \mathbf{g}(\mathbf{x}) = \sum_{i=1}^{\infty} \mathbf{c}_i \varphi_{\lambda_i}(\mathbf{x}). \tag{3}$$

The vectors $\mathbf{c}$'s are called Koopman modes. Under the action of $\mathcal{K}$, the above equation using (2) becomes

$$\mathbf{F}(\mathbf{x}) = \sum_{i=1}^{\infty} \lambda_i \mathbf{c}_i \varphi_{\lambda_i}(\mathbf{x}). \tag{4}$$

Thus, $\mathbf{F}$ expressed as a linear combination of the Koopman eigenfunctions $\{\varphi_{\lambda_i}\}_{i=1}^{\infty}$ reveals that the dynamics along each of the eigenfunctions is solely dictated by the corresponding eigenvalue. [1] To compute the ROA, we leverage the fact that eigenfunctions with 'large' corresponding eigenvalues largely describe $\mathbf{F}$ and the resulting dynamics.

B. Finite-Dimensional Approximation of Koopman Operators

Infinite-dimensionality of the Koopman operator $\mathcal{K}$ and its associated spectrum described by $\{\lambda_i, \varphi_{\lambda_i}\}_{i=1}^{\infty}$ make it challenging to compute these objects and utilize them to characterize the ROA. Naturally, one seeks a finite-dimensional approximation.

[1] Implicit in the above description is the assumption that $\mathcal{K}$ has a countable spectrum. See [32], [33] for a discussion on cases where $\mathcal{K}$ may have a continuous spectrum.

Consider a collection of dictionary functions

$$\mathbf{\Psi} := [\psi_1(\mathbf{x}), \ldots, \psi_D(\mathbf{x})]^{\mathrm{T}}, \tag{5}$$

where $\psi_i : \mathbb{R}^n \to \mathbb{C}$ for $i = 1, \ldots, D$. If the dictionary functions are rich enough to express the (dominant) eigenfunctions of $\mathcal{K}$ as their linear combinations, then the system dynamics in the span of $\mathbf{\Psi}$ should also be (roughly) describable via a linear map. Consider an observable g in the span of $\mathbf{\Psi}$ defined via the weights $\mathbf{b}$ as

$$g(\mathbf{x}) := \mathbf{\Psi}(\mathbf{x})^{\mathrm{T}}\mathbf{b}.$$

If the span of $\mathbf{\Psi}$ approximates $\mathbb{G}$ well, then g under the Koopman operator must be close to the span of $\mathbf{\Psi}$ expressed via the weights $\mathbf{Kb}$ for a suitable matrix $\mathbf{K} \in \mathbb{C}^{D\times D}$. In other words, we must have

$$g(\mathbf{F}(\mathbf{x})) \approx \mathbf{\Psi}(\mathbf{x})^{\mathrm{T}}\mathbf{Kb}.$$

The extended dynamic mode decomposition (EDMD) algorithm in [7] therefore seeks to identify the linear dynamics described by $\mathbf{K}$ and aims to minimize

$$J(\mathbf{K}) := \|\mathbf{\Psi}(\mathbf{F}(\mathbf{x}))^{\mathrm{T}}\mathbf{b} - \mathbf{\Psi}(\mathbf{x})^{\mathrm{T}}\mathbf{Kb}\|_2^2 \tag{6}$$

for arbitrary $\mathbf{b}$. Given a series of tuples

$$(\mathbf{x}^1, \mathbf{F}(\mathbf{x}^1)), \ldots, (\mathbf{x}^M, \mathbf{F}(\mathbf{x}^M))$$

composed of a state and its one-step propagation through the system dynamics $\mathbf{F}$, EDMD attempts to solve the data-driven variant of (6), the following least squares problem.

$$\underset{\mathbf{K}\in\mathbb{C}^{D\times D}}{\text{Minimize}} \sum_{j=1}^{M} \|\mathbf{\Psi}(\mathbf{F}(\mathbf{x}^j))^{\mathrm{T}}\mathbf{b} - \mathbf{\Psi}(\mathbf{x}^j)^{\mathrm{T}}\mathbf{Kb}\|_2^2. \tag{7}$$

Since the approximate linearity in the span of $\mathbf{\Psi}$ must hold for arbitrary observables (i.e., for all $\mathbf{b}$'s), one can therefore solve the following least squares problem.

$$\underset{\mathbf{K}\in\mathbb{C}^{D\times D}}{\text{Minimize}} \|\mathbf{Y} - \mathbf{XK}\|_F^2, \tag{8}$$

where $\|\cdot\|_F$ denotes the Frobenius norm and

$$\mathbf{X} := \frac{1}{M}\sum_{j=1}^{M} \mathbf{\Psi}(\mathbf{x}^j)\mathbf{\Psi}(\mathbf{x}^j)^{\mathrm{T}},$$

$$\mathbf{Y} := \frac{1}{M}\sum_{j=1}^{M} \mathbf{\Psi}(\mathbf{x}^j)\mathbf{\Psi}(\mathbf{F}(\mathbf{x}^j))^{\mathrm{T}}.$$

Indeed, $\mathbf{K}$ defines the finite-dimensional approximation to the Koopman operator $\mathcal{K}$. The eigenfunctions of the approximate operator are then given by

$$\varphi_{\lambda_i}(\mathbf{x}) = \mathbf{\Psi}(\mathbf{x})^{\mathrm{T}}\mathbf{v}_i, \tag{9}$$

where $\mathbf{v}_i$ is the i-th right eigenvector of $\mathbf{K}$ with eigenvalue λ_i. The least squares problem in (8) admits a closed-form solution, given by $\mathbf{X}^{\dagger}\mathbf{Y}$, where $\dagger$ stands for pseudoinverse.

Two remarks are in order. First, the quality of approximation of $\mathcal{K}$ by $\mathbf{K}$ depends on the choice of dictionary functions $\mathbf{\Psi}$. Radial basis functions and Hermite polynomials have appeared in the literature as good candidates, e.g., see [7]. An interesting alternative is advocated by [34]–[36], where they minimize the objective in (8) over $\mathbf{K}$ as well as $\mathbf{\Psi}$, where the latter is

represented parametrically via deep neural networks. Second, $\mathbf{K}$ can be updated in an online fashion, where the M tuples $(\mathbf{x}^i, \mathbf{F}(\mathbf{x}^i)), i = 1, \ldots, M$ are processed one at a time or in batches using recursive least squares. See [37] for details.

III. Estimating Region of Attraction

We leverage the approximate Koopman operator $\mathbf{K}$ derived using EDMD and propose a method to estimate the ROA of a dynamical system. Starting from $\mathbf{x}_0$, the system trajectory using (4) is given by

$$\mathbf{x}_t = \sum_{i=1}^{\infty} \lambda_i^t \mathbf{c}_i \varphi_{\lambda_i}(\mathbf{x}_0). \tag{10}$$

If λ_1 is the eigenvalue of $\mathcal{K}$ with the largest modulus, then we infer from the above relation that

$$\mathbf{x}_t \approx \lambda_1^t \mathbf{c}_1 \varphi_{\lambda_1}(\mathbf{x}_0) \tag{11}$$

for large t. In other words, the dominant eigenvalue largely dictates the dynamics over a long time-horizon. The relation in (11) also implies that any spatial variation of the dominant eigenfunction across the state space gets amplified through time. That is, one expects different behavior of the system in the long run, starting from two different points, if $|\varphi_{\lambda_1}|$ takes appreciably different values at these initial points. System trajectories starting from an initial point within the ROA will ultimately converge to the equilibrium point of the dynamics. Hence, one expects $|\varphi_{\lambda_1}|$ to be roughly the same over the ROA and exhibit sharp changes across its boundary. We propose to compute the boundary of the ROA by identifying such sharp changes in the modulus of the dominant eigenfunction of the approximate Koopman operator $\mathbf{K}$. We take a naive approach to compute such a boundary in

$$\partial\mathsf{ROA} := \{\mathbf{x} \in \mathbb{X} \ : \ |\varphi_{\lambda_1}(\mathbf{x})| = \bar{\varphi}\}, \tag{12}$$

where

$$\bar{\varphi} := \frac{1}{M} \sum_{j=1}^{M} |\varphi_{\lambda_1}(\mathbf{x}^j)|$$

is calculated from data. Here, ∂ROA stands for the boundary of the estimated ROA. The technique described here is inspired by the discussions in [38, Section 2.2]. [2]

The current technique to estimate the ROA boundary lacks any theoretical guarantees. The focus of our work is in showcasing the use of Koopman eigenfunctions for ROA estimation in power systems. A more theoretically grounded approach is left for a future endeavor. The efficacy of this scheme relies on two factors:

- the richness of the dictionary functions that dictates how well $\mathbf{K}$ approximates $\mathcal{K}$, and
- the sampling strategy of the M points, and whether they span points both in and out of the ROA.

IV. Numerical Results on 3-bus Power System

We now utilize the scheme outlined in the last two sections to compute the ROA of a 3-bus power system, and demonstrate possible applications of that computation. We consider a two-machine infinite-bus power system, the one-line diagram of which is given in Figure 1. Its electromechanical dynamics is described by the classical second-order synchronous generator model [39]:

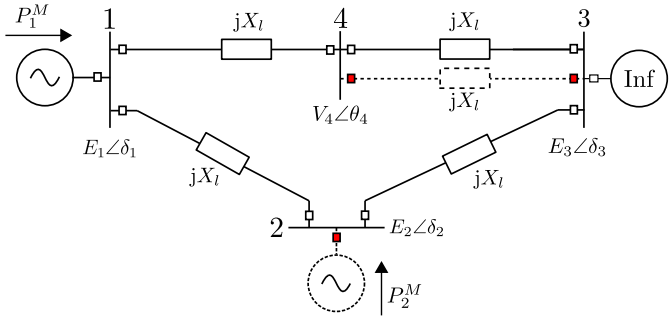

Fig. 1. The two machine infinite bus power system used for our numerical experiments are shown. The systems consists of two synchronous generators at buses 1 and 2 connected to the infinite-bus at bus 3. Red rectangles are circuit breakers that are opened to isolate faults that we study.

$$\begin{aligned} \frac{d\delta_i}{d\tau} &= \omega_i - \omega_s, \\ M_i \frac{d\omega_i}{d\tau} &= P_i^M - \sum_{j \in N_i} \frac{E_i E_j}{X_{ij}} \sin(\delta_i - \delta_j) - D_i(\omega_i - \omega_s). \end{aligned} \tag{13}$$

Here, δ_i and ω_i are the angle and angular frequency of the i-th generator, M_i is an inertia constant, D_i is a damping constant, P_i^M is a mechanical power input, ω_s is the system frequency, X_{ij} is a line reactance between bus i and j, and N_i collects the indices of all neighboring generator buses connected to the i-th generator bus. Values for the model parameters are provided in the appendix.

We compute the ROAs for two different faults:

- The synchronous generator at bus 2 malfunctions, and its machine starts slowing down at some time $\tau < 0\,[\mathrm{s}]$. Assume that it is isolated from the network at $\tau = 0\,[\mathrm{s}]$ by opening the circuit breaker at generator bus 2.
- The transmission line between buses 3 and 4 (denoted by the dotted line) has a balanced three-phase line-to-ground fault at some time $\tau < 0\,[\mathrm{s}]$, and is cleared at $\tau = 0\,[\mathrm{s}]$ by opening the circuit breakers located at buses 3 and 4.

1) Sampling data points: To compute the ROA, we perform numerical integration of the model in (13) with a time step $\Delta = 0.1\,[\mathrm{s}]$ from $\tau = 0\,[\mathrm{s}]$ to $\tau = 1\,[\mathrm{s}]$ for 2000 randomly-chosen initial points within the range $|\delta_i - \delta_i^{\mathrm{eq}}| \leq \pi + 1\,[\mathrm{rad}]$ and $|\omega_i - \omega_s| \leq 40\,[\mathrm{rad/s}]$. Any points beyond $\delta_i \geq 2\pi\,[\mathrm{rad}]$ are neglected.

2) Choice of dictionary functions: Following [7], [9], we choose 2000 radial basis functions (RBFs) of the form:

$$\psi_i(\mathbf{x}) = ||\mathbf{x} - \mathbf{x}_i^0||^2 \ln\left(||\mathbf{x} - \mathbf{x}_i^0||\right), \tag{14}$$

where $\mathbf{x}_i^0$ defines the 'center' of the i-th dictionary function. The centers are chosen via k-means clustering with $k = 2000$ on the data $\mathbf{x}^1, \ldots, \mathbf{x}^M$ with $M = 14611$ (for generator-fault) and $M = 16519$ (for line-fault). If a center coincides with a data point $\mathbf{x}^i$, we perturb it to avoid numerical issues.

[2] One can alternately utilize the magnitude of the gradient of the dominant eigenfunction. Other eigenfunctions may also prove useful for ROA characterization. A detailed numerical exploration is left for future work.

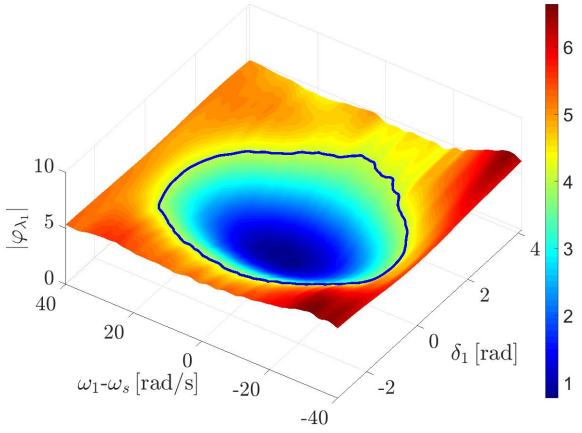

(a)

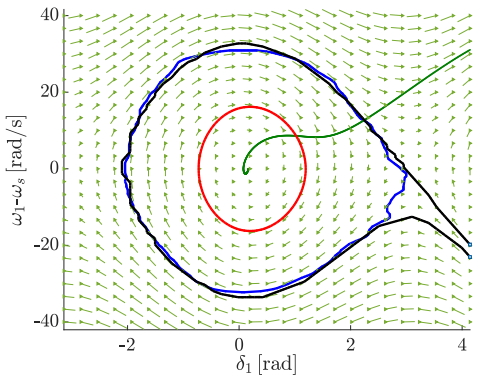

(b)

Fig. 2. The contour plot of $|\varphi_{\lambda_1}|$ is shown in (a). It also plots the boundary of the ROA in blue, where $|\varphi_{\lambda_1}| = \bar{\varphi}$. In (b), we plot the exact ROA in black, the estimated ROA from our method in blue, and the estimated ROA using polynomial optimization approach of [27] in red. The green line depicts the fault-on trajectory. All results pertain to the dynamics under generator malfunction.

A. Results on generator malfunction

Our experiments yield the dominant eigenvalue $\lambda_1 = 0.9894$ for the approximate Koopman operator, and the threshold $\bar{\varphi} = 4.0871$. Figure 2(a) illustrates the resulting ROA, and how the dominant eigenfunction exhibits a sharp change across its boundary, drawn in blue. Figure 2(b) demonstrates that the ROA estimated via the proposed method is much less conservative when compared to that obtained using polynomial optimization in [24], [27] and is also closer to the true ROA computed via exhaustive numerical integration. Accurate estimation of ROA is crucial in many applications. For example, ROAs are useful to compute critical clearing times (CCTs) of various faults, that in turn dictate relay settings for circuit breakers. Using the fault-on trajectory shown in Figure 2(b), EDMD yields a CCT of $0.397\,[\text{s}]$ that is close to the actual CCT of $0.398\,[\text{s}]$. Our results from EDMD are much less conservative compared to polynomial optimization that yields a CCT of $0.265\,[\text{s}]$, that is roughly 33% smaller than the true CCT. Our current approach to ROA estimation is sensitive to the portion of the state space we sample the initial points from. A better thresholding of the eigenfunction for ROA identification will prove useful.

We leave a remark on the polynomial optimization approach to ROA estimation. It begins by approximating the system dynamics $\mathbf{F}$ using polynomial functions of the states. Then, it seeks to maximize the size of a set over which a polynomial Lyapunov-style function decreases along the approximated system trajectories. That set provides an inner approximation of the ROA. Polynomial optimization problems can be solved via a hierarchy of semidefinite programs of increasing problem size. In theory, this hierarchy solves the optimization problem asymptotically. However, problem sizes quickly become prohibitively large, and only a few levels of the hierarchy can be numerically explored even for a relatively small power system such as in Figure 1. The estimated ROA in Figure 2 is derived with the same parameters as in [27]. The lack of scalability of this approach for practical power system operations, in part, motivated our current work. Our results encourage a detailed study on the viability of Koopman operators to reveal ROA for power system dynamics.

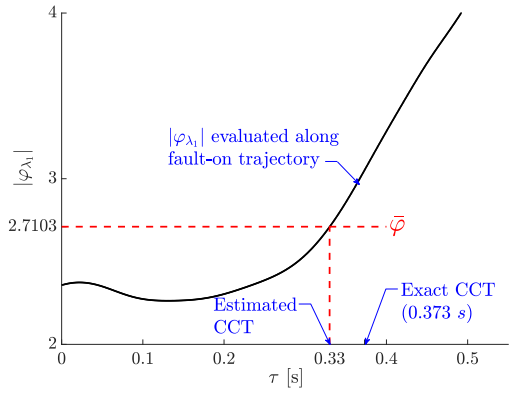

Fig. 3. The values of $|\varphi_{\lambda_1}|$ along the fault-on trajectory are drawn. CCT is evaluated at the point where $|\varphi_{\lambda_1}|$ passes $\bar{\varphi}$. Estimated CCT from our method and the exact CCT are indicated.

B. Results on three-phase line fault

For the line fault, the leading eigenvalue is $\lambda_1 = 0.9738$ and the threshold is given by $\bar{\varphi} = 2.7103$. Using the trajectory of $|\varphi_{\lambda_1}|$ in Figure 3, we infer a CCT of $0.330\,[s]$, that is close to the exact value $0.373\,[s]$ found by repeated simulations.

V. Concluding Remarks & Future Work

This paper reveals the use of a linear operator-theoretic framework to estimate the region of attraction for the nonlinear dynamical system model of a power-system. The estimation relies on the computation of an approximate Koopman operator. The spectrum of this operator contains the information useful to ROA estimation. Such an estimation is useful to estimate CCTs of various fault scenarios.

Our ultimate goal is to use the spectrum of Koopman operators within an online stability monitoring scheme. In this scheme, an offline calculation first estimates an ROA from a large data-set using the Koopman operator framework. Then, the approximate Koopman operator is updated over time

using recursive least squares with new datapoints generated from a model description, estimated from real measurements. The current work defines the first step in that direction. We plan to contrast such a scheme against other online stability assessment, e.g., proposed in [40], [41], in terms of accuracy and scalability. An important challenge in generalizing our technique for large power system examples lies in the identification of a rich set of dictionary functions for which neural networks along the lines of [34] can prove useful.

Our proposed approach lacks theoretical guarantees, e.g., one can overestimate CCTs using our method. Our numerical results encourage us to pursue more theoretically grounded approaches to ROA estimation for powers systems with provable guarantees leveraging Koopman operator theory.

VI. Appendix

The parameters for the experiments on the Two-Machine Infinite-Bus power system in Figure 1 are given by: system angular frequency $\omega_s = 120\pi\,[\mathrm{rad}\cdot\mathrm{s}^{-1}]$, inertia constant $M_{1,2} = 0.0159\,[\mathrm{rad}^{-1}\mathrm{s}^2]$, machine damping $D_{1,2} = 0.0053\,[\mathrm{rad}^{-1}\mathrm{s}]$, machine terminal voltage $E_{1\sim3} = 1\,[\mathrm{pu}]$, infinite-bus angle $\delta_3 = 0\,[\mathrm{rad}]$, mechanical power input $P_1^M = 1$, $P_2^M = 0.6\,[\mathrm{pu}]$, and line impedance $X_l = 0.2\,[\mathrm{pu}]$.

References

[1] J. v. Neumann and B. Koopman, "Dynamical systems of continuous spectra," *Proceedings of the National Academy of Sciences of the United States of America*, vol. 18, no. 3, pp. 255–263, Mar 1932.

[2] A. Lasota and M. C. Mackey, *Chaos, Fractals, and Noise: Stochastic Aspects of Dynamics*, ser. Applied Mathematical Sciences. Springer-Verlag New York, 1994.

[3] U. Vaidya and P. G. Mehta, "Lyapunov measure for almost everywhere stability," *IEEE Transactions on Automatic Control*, vol. 53, pp. 307–323, 2008.

[4] I. Mezić, "Spectral properties of dynamical systems, model reduction and decompositions," *Nonlinear Dynamics*, vol. 41, no. 1-3, pp. 309–325, 2005.

[5] A. Mauroy and I. Mezić, "Global stability analysis using the eigenfunctions of the koopman operator," *IEEE Transactions on Automatic Control*, vol. 61, no. 11, pp. 3356–3369, Nov 2016.

[6] M. Budišić, R. Mohr, , and I. Mezić, "Applied koopmanism," *Chaos: An Interdisciplinary Journal of Nonlinear Science*, vol. 22, no. 4, p. 047510, Dec 2012.

[7] M. O. Williams, I. G. Kevrekidis, and C. W. Rowley, "A data–driven approximation of the koopman operator: Extending dynamic mode decomposition," *Journal of Nonlinear Science*, vol. 25, no. 6, pp. 1307–1346, Dec 2015.

[8] J. H. Tu, C. W. Rowley, D. M. Luchtenburg, S. L. Brunton, and J. N. Kutz, "On dynamic mode decomposition: Theory and applications," *Journal of Computational Dynamics*, vol. 1, p. 391, 2014.

[9] J. N. Kutz, S. L. Brunton, B. W. Brunton, and J. L. Proctor, *Dynamic Mode Decomposition*. Philadelphia, PA: Society for Industrial and Applied Mathematics, 2016.

[10] P. Varaiya, F. F. Wu, and R.-L. Chen, "Direct methods for transient stability analysis of power systems: Recent results," *Proceedings of the IEEE*, vol. 73, no. 12, pp. 1703–1715, Dec 1985.

[11] M. A. PAI, "Survey of practical direct methods of stability analysis in power systems," *Electric Machines & Power Systems*, vol. 9, no. 2-3, pp. 131–143, 1984.

[12] P. W. Sauer, M. A. Pai, and J. H. Chow, *Power System Dynamics and Stability: With Synchrophasor Measurement and Power System Toolbox*. John Wiley & Sons, 2017.

[13] H. Khalil, *Nonlinear Systems*, 3rd ed., P. Hall, Ed. Upper Saddle River, NJ: Prentice Hall, 2002.

[14] P. A. Parrilo, "Structured semidefinite programs and semialgebraic geometry methods in robustness and optimization," Tech. Rep., 2000.

[15] A. Fouad and V. Vittal, *Power System Transient Stability Analysis Using the Transient Energy Function Method*. Pearson Education, 1991.

[16] H. Chiang, *Direct Methods for Stability Analysis of Electric Power Systems: Theoretical Foundation, BCU Methodologies, and Applications*. Wiley, 2011.

[17] M. A. Pai, *Power System Stability: Analysis by the Direct Method of Lyapunov*, ser. North-Holland systems and control series. North-Holland Publishing Company, 1981.

[18] A. Pai, *Energy Function Analysis for Power System Stability*. Springer US, 1989.

[19] Y. Zou, M.-H. Yin, and H.-D. Chiang, "Theoretical foundation of the controlling UEP method for direct transient-stability analysis of network-preserving power system models," *IEEE Transactions on Circuits and Systems I: Fundamental Theory and Applications*, vol. 50, no. 10, pp. 1324–1336, Oct 2003.

[20] R. T. Treinen, V. Vittal, and W. Kliemann, "An improved technique to determine the controlling unstable equilibrium point in a power system," *IEEE Transactions on Circuits and Systems I: Fundamental Theory and Applications*, vol. 43, no. 4, pp. 313–323, April 1996.

[21] H. D. Chiang and J. S. Thorp, "The closest unstable equilibrium point method for power system dynamic security assessment," *IEEE Transactions on Circuits and Systems*, vol. 36, no. 9, pp. 1187–1200, Sept 1989.

[22] C.-W. Liu and J. S. Thorp, "A novel method to compute the closest unstable equilibrium point for transient stability region estimate in power systems," *IEEE Transactions on Circuits and Systems I: Fundamental Theory and Applications*, vol. 44, no. 7, pp. 630–635, July 1997.

[23] H. Chiang, J. Tong, and Y. Tada, "On-line transient stability screening of 14,000-bus models using TEPCO-BCU: Evaluations and methods," in *IEEE PES General Meeting*, July 2010, pp. 1–8.

[24] M. Anghel, F. Milano, and A. Papachristodoulou, "Algorithmic construction of Lyapunov functions for power system stability analysis," *IEEE Transactions on Circuits and Systems I: Regular Papers*, vol. 60, no. 9, pp. 2533–2546, Sept 2013.

[25] W. Tan and A. Packard, "Stability region analysis using polynomial and composite polynomial Lyapunov functions and sum-of-squares programming," *IEEE Transactions on Automatic Control*, vol. 53, no. 2, pp. 565–571, Mar 2008.

[26] G. Franze, D. Famularo, and A. Casavola, "Constrained nonlinear polynomial time-delay systems: A sum-of-squares approach to estimate the domain of attraction," *IEEE Transactions on Automatic Control*, vol. 57, no. 10, pp. 2673–2679, Oct 2012.

[27] H. Choi, P. J. Seiler, and S. V. Dhople, "Robust power systems stability assessment with sum of squares optimization," in *2015 IEEE Power Energy Society General Meeting*, July 2015, pp. 1–5.

[28] Y. Susuki and I. Mezić, "Nonlinear koopman modes and power system stability assessment without models," *IEEE Transactions on Power Systems*, vol. 29, no. 2, pp. 899–907, March 2014.

[29] Y. Susuki and I. Mezic, "Nonlinear koopman modes and a precursor to power system swing instabilities," *IEEE Transactions on Power Systems*, vol. 27, no. 3, pp. 1182–1191, Aug 2012.

[30] F. Dorfler and F. Bullo, "Kron reduction of graphs with applications to electrical networks," *IEEE Transactions on Circuits and Systems I: Regular Papers*, vol. 60, no. 1, pp. 150–163, Jan 2013.

[31] P. Sauer and M. Pai, *Power System Dynamics and Stability*. Stipes Publishing L.L.C., 2006.

[32] I. Mezić, "Koopman operator spectrum and data analysis," *arXiv:1702.07597*, 2017.

[33] B. Lusch, J. N. Kutz, and S. L. Brunton, "Deep learning for universal linear embeddings of nonlinear dynamics," *arXiv:1712.09707v2*, 2018.

[34] E. Yeung, S. Kundu, and N. O. Hodas, "Learning deep neural network representations for Koopman operators of nonlinear dynamical systems," *arXiv preprint arXiv:1708.06850*, 2017.

[35] B. Lusch, J. N. Kutz, and S. L. Brunton, "Deep learning for universal linear embeddings of nonlinear dynamics," *arXiv preprint arXiv:1712.09707*, 2017.

[36] Q. Li, F. Dietrich, E. Bollt, and I. G. Kevrekidis, "Extended dynamic mode decomposition with dictionary learning: A data-driven adaptive spectral decomposition of the Koopman operator," vol. 27, 07 2017.

[37] H. Zhang, C. W. Rowley, E. A. Deem, and L. N. Cattafesta, "Online dynamic mode decomposition for time-varying systems," *arXiv:1707.02876*, vol. abs/1707.02876, 2017.

[38] A. Mauroy, I. Mezić, and J. Moehlis, "Isostables, isochrons, and koopman spectrum for the action–angle representation of stable fixed point dynamics," *Physica D: Nonlinear Phenomena*, vol. 261, pp. 19–30, 2013.

[39] J. D. D. Glover and M. S. Sarma, *Power System Analysis and Design*, 3rd ed. Pacific Grove, CA, USA: Brooks/Cole Publishing Co., 2001.

[40] J. Yan, C. Liu, and U. Vaidya, "A PMU-based monitoring scheme for rotor angle stability," in *2012 IEEE Power and Energy Society General Meeting*, July 2012, pp. 1–5.

[41] S. Dasgupta, M. Paramasivam, U. Vaidya, and V. Ajjarapu, "Real-time monitoring of short-term voltage stability using PMU data," *IEEE Transactions on Power Systems*, vol. 28, no. 4, pp. 3702–3711, Nov 2013.